Finite deformation plasticity based on the additive split of the rate of deformation and hyperelasticity

Jacob Fish and Kamlun Shek[1]
Departments of Civil and Mechanical Engineering
Rensselaer Polytechnic Institute
Troy, NY 12180

Abstract

Finite deformation plasticity formulation based on additive split of rate of deformation and hyperelasticity is presented. This approach is valid for finite elastic and plastic strains, while rendering the choice and numerical integration of objective stress rates superfluous as the results are automatically objective. For small elastic strains our method reduces to the classical hypoelastic-corotational formulation provided that the Dienes objective stress rate is employed, while in the absence of inelastic deformation it coincides with the hyperelastic formulation. The validity of the model has been examined on four test problems and the numerical results were found to be in good agreement with either the exact solution or experimental data.

1.0 Introduction

The proper formulation of finite deformation elastoplastic kinematics, elastic response and the flow rule has been a subject of considerable conjecture. One of the major difficulties stems from the coupling between elastic and plastic properties. It is well known that initially elastically isotropic material may become elastically anisotropic due to plastic flow, which means that Helmholtz free energy density is not only a function of elastic deformation but has some dependency on the plastic flow. Fortunately, for moderate plastic deformation (up to 30% [12][13]), dislocations and other lattice defects caused by plastic flow, have a negligible effect on the deformation of crystal lattice which governs elastic constants. This has been realized by many practitioners, who observed that elastic constants are not appreciably affected by manufacturing processes involving plastic forming, nor has the elastic deformation a profound influence on the plastic flow.

Finite elastoplastic kinematics is another issue of considerable debate. For example, based on the energy conservation principle, Nemat-Nasser [26] has shown that the rate of deformation, $\boldsymbol{d}$, decomposes additively as

$$\boldsymbol{d} = {}_e\boldsymbol{d} + {}_p\boldsymbol{d} \tag{1}$$

for finite elastic (e) and plastic (p) rate of deformation provided that the strain increments are defined with respect to the same reference configuration. Green and Naghdi [10], have argued that an additive decomposition of Lagrangian strain, $\boldsymbol{E}$

1. Current address: The Goodyear Tire and Rubber Company, D/431A, Akron, OH 44309

$$\boldsymbol{E} = {}_e\boldsymbol{E} + {}_p\boldsymbol{E} \tag{2}$$

into elastic-plastic components is supported by solid thermodynamic principles. Lee [20][21] advocated a theory based on multiplicative decomposition of the deformation gradient, $\boldsymbol{F}$

$$\boldsymbol{F} = {}_e\boldsymbol{F}\,{}_p\boldsymbol{F} \tag{3}$$

where the elastic deformation gradient, ${}_e\boldsymbol{F}$, is obtained by independently unloading infinitesimal volume elements of the body into an intermediate configuration defined by this collection of unloaded elements. It is important to realize that the three theories are fundamentally different, i.e., if one, for example, adopts multiplicative decomposition, then it is a trivial exercise to show that neither additive decomposition holds, and vice versa. In an attempt to reconcile these different kinematical assumptions, ${}_e\boldsymbol{E}$ [11][31] and ${}_e\boldsymbol{d}$ [26] have been interpreted as mixed elasto-plastic deformation tensors.

Other kinematical splits can be found in the literature. Nemat-Nasser advocated an additive split of the deformation gradients [26], as well as the multiplicative decomposition, where the order of plastic and elastic deformation gradients in (3) is interchanged [25]. Kim and Oden [19], on the other hand, suggested decomposing the stretch tensor additively.

Even though there is no consensus with respect to the most favorable finite elastoplastic kinematics, numerical algorithms developed in the past 15 years have been primarily focussing on the following two approaches:

Category 1: Multiplicative hyperelastic plasticity

This class of methods is based on multiplicative elasto-plastic kinematics (3), hyperelasticity and the existence of Helmholtz free energy density governed by either elasto-plastic deformation [7][19][23][25][28][29][34][35][36][39], or elastic deformation only [2][21]. The latter, as well as an additive split of the Helmholtz free energy density [7][8], are computationally attractive as they permit computation of stresses based on the elastic deformation only.

Category 2: Rate-additive hypoelastic plasticity

This approach hinges on the additive decomposition of the rate of deformation (1), hypoelasticity, and objective stress rates. Special care is exercised in the integration of rate constitutive equations to preserve objectivity [4][15][17][27]. Even though these type of methods are very attractive from the computational point of view [1][3], they are limited to small elastic strains (but large rotations) for which the hypothesis of hypoelasticity is valid. Moreover, they suffer from a somewhat adhoc choice of objective stress rates. Nevertheless, the *rate-additive hypoelastic* approach is appropriate for most of the engineering materials including metals, where elastic strains remain small and thus differences in the formulation of elastic response have little or no effect on the computed solution. On the

other hand, for some polymers exhibiting significant elastic and plastic deformation of comparable magnitude, a different treatment is required.

The primary objectives of the present manuscript are threefold:

(i) In an attempt to capitalize on the generality of the *multiplicative-hyperelastic approach* and the computational efficiency of the *rate-additive-hypoelastic* approach, we present a hybrid formulation based on the additive split of the rate of deformation and hyperelasticity. Such an approach, referred hereafter as the *rate-additive-hyperelastic* approach, remains valid for finite elastic and plastic strains, while rendering the choice and numerical integration of objective stress rates superfluous as the results are automatically objective.

(ii) We show that in the case of small elastic strains the rate-additive-hyperelastic formulation reduces to the hypoelastic-corotational formulation [4][15][18], provided that the Dienes [5] objective stress rate is employed. Furthermore, our formulation reduces to the hyperelastic formulation in the absence of inelastic deformation. This suggests that the magnitude of elastic and plastic deformation (characterized by an appropriate norm) can be used as an indicator for appropriate model selection.

(iii) The validity of the model will be examined for the following four problems: (a) Axial tension-rigid body rotation of a hyperelastic-plastic bar for which the exact solution can be easily obtained, (b) the classical simple shear problem [24], which reveals spurious oscillatory shear stress behavior for certain types of objective stress rates, (c) the torsion problem of the hollow cylinder [32] for which the axial strains have been observed to be two orders of magnitude smaller than those of shear strains, and (d) the axisymmetric expansion of an elasto-plastic thick-walled cylinder for which the exact solution has been reported in [6].

The manuscript is organized as follows. Section 2 examines hyperelasticity and hypoelasticity within the framework of corotational formulation and shows that for infinitesimal elastic stretches the two theories coincide for a certain choice of corotational frame. Stress integration schemes and the derivation of the consistent tangent stiffness matrix for the *rate-additive-hyperelastic* approach are presented in Section 3. Numerical examples conclude the manuscript.

2.0 Hypoelasticity versus hyperelasticity

As a prelude to the finite deformation plasticity incorporating additive split and hyperelasticity, we start by summarizing the basic hypoelasticity and hyperelasticity equations with the intent of deriving the relation between the two formulations.

2.1 Hypoelastic corotational formulation

Consider two neighboring particles of the body situated at points H and Q in the undeformed configuration such that the unit vector, denoted as $\boldsymbol{B}$, is pointing from Q to H as

shown in Figure 1. The particles originally positioned at points *H* and *Q* move to the positions *h* and *q*, respectively, with the corresponding unit vector $\boldsymbol{b}$. The rotation between the two unit vectors can be written as

$$\boldsymbol{b} = \Re \cdot \boldsymbol{B}$$

where $\Re$ is orthogonal such that $\Re \cdot \Re^T = \mathbf{I}$, and $\mathbf{I}$ represents an identity matrix.

The rate of rotation is given by

$$\dot{\boldsymbol{b}} = \dot{\Re} \cdot \boldsymbol{B} = \boldsymbol{W} \cdot \boldsymbol{b}.$$

where

$$\boldsymbol{W} = \dot{\Re} \cdot \Re^{-1}$$

Note that $\boldsymbol{W}$ coincides with the spin tensor if $\boldsymbol{b}$ is aligned along one of the principal directions of the rate of deformation tensor. We now focus on the corotational frame $\boldsymbol{x}^{\Re}$ which transforms with respect to the undeformed configuration as $\boldsymbol{x}^{\Re} = \Re \cdot \boldsymbol{X} + \text{constant}$. A family of the corotational Cauchy stress tensor, denoted as $\sigma^{\Re}$, can be defined as

$$\sigma^{\Re} = \Re^T \cdot \sigma \cdot \Re \tag{4}$$

The rate of $\sigma^{\Re}$ follows from the linearization of (4)

$$\begin{aligned}\dot{\sigma}^{\Re} &= \dot{\Re}^T \cdot \sigma \cdot \Re + \Re^T \cdot \dot{\sigma} \cdot \Re + \Re^T \cdot \sigma \cdot \dot{\Re} \\ &= \Re^T \cdot \boldsymbol{W}^T \cdot \sigma \cdot \Re + \Re^T \cdot \dot{\sigma} \cdot \Re + \Re^T \cdot \sigma \cdot \boldsymbol{W} \cdot \Re = \Re^T \cdot \overset{\triangledown}{\sigma} \cdot \Re\end{aligned}$$

or

$$\overset{\triangledown}{\sigma} = \Re \cdot \dot{\sigma}^{\Re} \cdot \Re^T \tag{5}$$

where $\overset{\triangledown}{\sigma}$ is the so called objective stress rate given by

$$\overset{\triangledown}{\sigma} = \dot{\sigma} - \boldsymbol{W} \cdot \sigma - \sigma \cdot \boldsymbol{W}^T$$

$\overset{\triangledown}{\sigma}$ can be interpreted as a rate of $\sigma^{\Re}$ expressed in the current frame. Since $\dot{\sigma}^{\Re}$ and $\overset{\triangledown}{\sigma}$ obey transformation rules for second order tensors, they are considered objective stress rate measures. Note $\dot{\sigma}$ does not obey transformation rules of second order tensors, and therefore, it is not objective.

For hypoelastic materials the constitutive equation is given by

$$\overset{\nabla}{\boldsymbol{\sigma}} = \boldsymbol{L} : \boldsymbol{d} \tag{6}$$

where $\boldsymbol{L}$ is the elasticity fourth order tensor and $\boldsymbol{d}$ is the rate of deformation defined as

$$\boldsymbol{d} \equiv \{\boldsymbol{l}\}_s \qquad \boldsymbol{l} \equiv \frac{\partial \boldsymbol{v}}{\partial \boldsymbol{x}}$$

and $\boldsymbol{v}$ represents the velocity field; $\boldsymbol{l}$ denotes the spatial velocity gradient, and $\{\bullet\}_s$ is a symmetrization operator.

Substituting (5) into (6), premultiplying and postmultiplying the result with $\mathfrak{R}^T$ and $\mathfrak{R}$ yields

$$\dot{\boldsymbol{\sigma}}^{\mathfrak{R}} = \mathfrak{R}^T \cdot (\boldsymbol{L} : \boldsymbol{d}) \cdot \mathfrak{R}$$

Let $\boldsymbol{d}^{\mathfrak{R}}$ denote the set of corotational rate of deformation tensors defined as

$$\boldsymbol{d}^{\mathfrak{R}} = \mathfrak{R}^T \cdot \boldsymbol{d} \cdot \mathfrak{R}$$

then the hypoelastic constitutive equation (6) in the corotational frame can be expressed as

$$\dot{\boldsymbol{\sigma}}^{\mathfrak{R}} = \boldsymbol{L}^{\mathfrak{R}} : \boldsymbol{d}^{\mathfrak{R}} \tag{7}$$

where $\boldsymbol{L}^{\mathfrak{R}}$ in the component form is given as

$$L^{\mathfrak{R}}_{ijkl} = \mathfrak{R}_{ai}\mathfrak{R}_{bj}\mathfrak{R}_{ck}\mathfrak{R}_{dl}L_{abcd} \tag{8}$$

It can be seen that the form of the constitutive equations in the corotational frame is identical to that in small deformation theory. Note that for isotropic materials the constitutive properties are rotation independent and thus $\boldsymbol{L}^{\mathfrak{R}} = \boldsymbol{L}$.

Clearly the constitutive equation (7) in the corotational frame is not unique. First, various choices of rotations, $\mathfrak{R}$, will ultimately yield different material responses. Secondly, what is a proper choice of $\boldsymbol{L}$? Can it be chosen the same as in small deformation theory? These questions are addressed in the next section, where the choice of $\mathfrak{R}$ and $\boldsymbol{L}$ is made to maintain consistency with the notion of hyperelasticity.

2.2 Hyperelastic corotational formulation

The constitutive equation for a hyperelastic solid can be written in the following form

$$\boldsymbol{S} = 2\frac{\partial \Psi}{\partial \boldsymbol{U}^2} = 2\frac{\partial \Psi}{\partial \boldsymbol{C}} \tag{9}$$

where Ψ is the Helmholtz free energy density function; $\boldsymbol{U}$ represents the right stretch tensor and $\boldsymbol{U}^2 = \boldsymbol{U}^T \cdot \boldsymbol{U}$; $\boldsymbol{C}$ is the Green deformation tensor where $\boldsymbol{C} = \boldsymbol{U}^2$; $\boldsymbol{S}$ denotes the second Piola-Kirchhoff stress tensor which is related to the Cauchy stress, σ, as

$$\boldsymbol{S} = J\boldsymbol{F}^{-1} \cdot \sigma \cdot \boldsymbol{F}^{-T} \tag{10}$$

where $\boldsymbol{F}$ represents the deformation gradient and J is the Jacobian which is defined as the determinant of $\boldsymbol{U}$. In the following we focus on the member of the corotational family of stresses by selecting the rotation tensor $\Re = \boldsymbol{R}$ from the polar decomposition $\boldsymbol{F} = \boldsymbol{R} \cdot \boldsymbol{U}$. Thus

$$\sigma^R \equiv \boldsymbol{R}^T \cdot \sigma \cdot \boldsymbol{R} = 2J^{-1}\boldsymbol{U} \cdot \frac{\partial \Psi}{\partial \boldsymbol{U}^2} \cdot \boldsymbol{U} \tag{11}$$

Taking the material time derivative of (11) gives

$$\dot{\sigma}^R = 2J^{-1}\left\{\dot{\boldsymbol{U}} \cdot \frac{\partial \Psi}{\partial \boldsymbol{U}^2} \cdot \boldsymbol{U} + \boldsymbol{U} \cdot \frac{d}{dt}\left(\frac{\partial \Psi}{\partial \boldsymbol{U}^2}\right) \cdot \boldsymbol{U} + \boldsymbol{U} \cdot \frac{\partial \Psi}{\partial \boldsymbol{U}^2} \cdot \dot{\boldsymbol{U}}\right\} + 2\frac{dJ^{-1}}{dt}\boldsymbol{U} \cdot \frac{\partial \Psi}{\partial \boldsymbol{U}^2} \cdot \boldsymbol{U} \tag{12}$$

To linearize the right stretch tensor we recall

$$\boldsymbol{l} = \dot{\boldsymbol{F}} \cdot \boldsymbol{F}^{-1} = \dot{\boldsymbol{R}} \cdot \boldsymbol{R}^T + \boldsymbol{R} \cdot \dot{\boldsymbol{U}} \cdot \boldsymbol{U}^{-1} \cdot \boldsymbol{R}^T$$

and defining the following corotational measures: $\boldsymbol{d}^R \equiv \boldsymbol{R}^T \cdot \boldsymbol{d} \cdot \boldsymbol{R}$, $\boldsymbol{w}^R \equiv \boldsymbol{R}^T \cdot \boldsymbol{w} \cdot \boldsymbol{R}$, $\Omega^R \equiv \boldsymbol{R}^T \cdot \Omega \cdot \boldsymbol{R}$, $\Omega \equiv \dot{\boldsymbol{R}} \cdot \boldsymbol{R}^T$, where $\boldsymbol{w} \equiv \{\boldsymbol{l}\}_a$ is an antisymmetric part of $\boldsymbol{l}$, the rate of the right strech tensor can be expressed as:

$$\dot{\boldsymbol{U}} = (\boldsymbol{d}^R + \boldsymbol{w}^R - \Omega^R) \cdot \boldsymbol{U} \qquad \text{or} \qquad \boldsymbol{d}^R = \{\dot{\boldsymbol{U}} \cdot \boldsymbol{U}^{-1}\}_s \tag{13}$$

The second term in (12) can be written as

$$\frac{d}{dt}\left(\frac{\partial \Psi}{\partial \boldsymbol{U}^2}\right) = \frac{\partial^2 \Psi}{\partial \boldsymbol{U}^2 \partial \boldsymbol{U}^2} : \frac{d\boldsymbol{U}^2}{dt} = \frac{\partial^2 \Psi}{\partial \boldsymbol{U}^2 \partial \boldsymbol{U}^2} : (2\boldsymbol{F}^T \cdot \boldsymbol{d} \cdot \boldsymbol{F}) = \frac{\partial^2 \Psi}{\partial \boldsymbol{U}^2 \partial \boldsymbol{U}^2} : (2\boldsymbol{U} \cdot \boldsymbol{d}^R \cdot \boldsymbol{U}) \tag{14}$$

Substituting (13), (14) with $\dot{J} = J\mathrm{tr}(\boldsymbol{d}^R)$ into (11) yields

$$\dot{\sigma}^R = \boldsymbol{L}^R : \boldsymbol{d}^R + \{\boldsymbol{h}^R \cdot \boldsymbol{e}^R\}_s \qquad \boldsymbol{e}^R = \boldsymbol{d}^R + \omega^R - \frac{1}{2}\mathrm{tr}(\boldsymbol{d}^R)\mathbf{I} \tag{15}$$

where $\omega^R = \boldsymbol{w}^R - \Omega^R$; $\boldsymbol{L}^R$ and $\boldsymbol{h}^R$ in the component form are given as

$$L^R_{ijkl}(\boldsymbol{U}) = \frac{4}{\det(\boldsymbol{U})} U_{ip}U_{jq}U_{kr}U_{ls}\frac{\partial^2\Psi}{\partial U^2_{pq}\partial U^2_{rs}}$$

$$h^R_{ij}(\boldsymbol{U}) = \frac{4}{\det(\boldsymbol{U})} U_{ik}U_{jl}\frac{\partial\Psi}{\partial U^2_{kl}}$$

It should be noted that for small elastic deformation, $\boldsymbol{U} \approx \mathbf{I}$, the following holds

$$\frac{\partial\Psi}{\partial \boldsymbol{U}^2} = O(\boldsymbol{U}-\mathbf{I}) \qquad J = O(1) \qquad \boldsymbol{h}^R = O(\boldsymbol{U}-\mathbf{I})$$

and hence (15) can be approximated as

$$\dot{\sigma}^R = 4\frac{\partial^2\Psi}{\partial \boldsymbol{U}^2\partial \boldsymbol{U}^2} : \boldsymbol{d}^R \tag{16}$$

Comparing (7) and (16), we conclude that in the case of small elastic deformation (but arbitrary rotations), the hyperelastic and hypoelastic formulations are identical provided that

$$\boldsymbol{L}^{\Re} = 4\frac{\partial^2\Psi}{\partial \boldsymbol{U}^2\partial \boldsymbol{U}^2} \qquad \text{and} \qquad \Re = \boldsymbol{R}$$

For more details on the corotational formulation see [4][37][38].

3.0 Finite deformation plasticity based on the additive split of the rate of deformation and hyperelasticity

3.1 Basic assumptions

In developing finite deformation elasto-plastic equations the primary criteria we shall adopt are as follows:

i. The finite deformation elasto-plastic rate relations should coincide with hyperelasticity in the absence of inelastic deformation.

ii. We postulate that the stress in finite deformation plasticity may be derived from Helmholtz free energy density [7][8]. Therefore, the corotational Cauchy stress can be written as

$$\sigma^R = \frac{2}{\det({}_e\boldsymbol{U})}\, {}_e\boldsymbol{U}\, \frac{\partial_e\Psi}{\partial_e \boldsymbol{U}^2}\, {}_e\boldsymbol{U} \tag{17}$$

analogous to (11). In other words, we assume that in a finitely deforming elasto-plastic solid, the objective relations are governed by (15), with the only exception that various strain and strain rate measures, such as $\boldsymbol{U}, \boldsymbol{d}^R$ are replaced by their elastic counterparts, ${}_e\boldsymbol{U}, {}_e\boldsymbol{d}^R$ whereas rotations are associated with elastic deformation only, i.e.,

$$\boldsymbol{w} = {}_e\boldsymbol{w} \qquad \boldsymbol{R} = {}_e\boldsymbol{R} \tag{18}$$

iii. Finally, we will adopt an additive split of the rate of the deformation tensor

$$\boldsymbol{d} = {}_e\boldsymbol{d} + {}_p\boldsymbol{d} \tag{19}$$

where the left subscripts e and p denote elastic and plastic deformation, respectively.

3.2 Governing equations

As previously hypothesized the stress in a finitely deforming elasto-plastic solid is derived from the elastic strain density function ${}_e\Psi$. Thus the rate of corotational Cauchy stress can be written, similar to (15), in terms of the elastic stretch ${}_e\boldsymbol{U}$ and the elastic corotational rate of deformation ${}_e\boldsymbol{d}^R$ as follows

$$\dot{\sigma}^R = \boldsymbol{L}^R({}_e\boldsymbol{U}) : {}_e\boldsymbol{d}^R + \{\boldsymbol{h}^R({}_e\boldsymbol{U}) \cdot {}_e\boldsymbol{e}^R\}_S \qquad {}_e\boldsymbol{e}^R = {}_e\boldsymbol{d}^R + \omega^R - \frac{1}{2}\mathbf{tr}({}_e\boldsymbol{d}^R)\mathbf{I} \ . \tag{20}$$

Since plastic strains are a nonlinear function of stresses, it is necessary to integrate the constitutive equations along the prescribed loading path in order to obtain the current stress state. In this section we present a simple, computationally efficient implicit procedure for the elasto-plastic stress updates. For simplicity of presentation, we adopt an elasto-plastic material with isotropic elastic properties obeying von Mises yield function with a linear combination of isotropic and kinematic hardening [15].

Consider the yield function of the following form

$$\phi \equiv \bar{\sigma}^R - Y \tag{21}$$

in which Y is the yield stress of the material in the uniaxial test which evolves according to the hardening laws assumed; $\bar{\sigma}^R$ is the effective stress defined as

$$\bar{\sigma}^R \equiv \sqrt{\frac{3}{2}\xi^R : \boldsymbol{P} : \xi^R} \qquad \xi^R \equiv \sigma^R - \alpha^R$$

α^R corresponds to the center of the yield surface in the corotational deviatoric stress space. Evolution of corotational back stresses, $\alpha^R = \boldsymbol{R}^T \cdot \boldsymbol{\alpha} \cdot \boldsymbol{R}$, is assumed to follow the kinematic hardening rule. For von Mises plasticity, $\boldsymbol{P}$ is a projection operator which transforms a symmetric second order tensor from non-deviatoric space to deviatoric space, i.e.,

$$P_{ijkl} = \frac{1}{2}(\delta_{ik}\delta_{jl} + \delta_{il}\delta_{jk}) - \frac{1}{3}\delta_{ij}\delta_{kl}$$

For simplicity we adopt the associative flow rule

$$ {}_p\boldsymbol{d}^R = \dot{\lambda}\boldsymbol{P} : \xi^R \tag{22}$$

and the hardening evolution law [15] in the context of isotropic, homogeneous, elasto-plastic media. A scalar, material dependent parameter β where $0 \le \beta \le 1$ is used as a measure of the proportion of isotropic and kinematic hardening with λ as a plastic parameter determined by the consistency condition. Accordingly, the evolution of Y and α^R can be expressed in the following rate forms:

$$\dot{\alpha}^R = \frac{2}{3}\dot{\lambda}(1-\beta)H\boldsymbol{P} : \xi^R \tag{23}$$

$$\dot{Y} = \beta H\, {}_p\bar{d}^R \tag{24}$$

where ${}_p\bar{d}^R$ is the corotational effective plastic rate of deformation defined as

$$ {}_p\bar{d}^R \equiv \sqrt{\frac{2}{3}\, {}_p\boldsymbol{d}^R : {}_p\boldsymbol{d}^R} \tag{25}$$

While $\beta = 0$ refers to pure isotropic hardening, $\beta = 1$ is merely the widely used Ziegler-Prager kinematic hardening rule [33] for metals without isotropic hardening. H is a hardening parameter defined as the ratio between effective stress rate to effective plastic rate of deformation.

3.3 Stress update procedure

In a typical load step $n+1$, the new configuration can be expressed as a sum of the configuration at the previous load step n and the displacement increment $\Delta\boldsymbol{u}$:

$$ {}^{n+1}\boldsymbol{x} = {}^{n}\boldsymbol{x} + \Delta\boldsymbol{u}$$

where the left superscript refers to the load step count with $n+1$ being the current step. Subsequently we omit the left superscript for the current step, such that all variables without the left superscripts refer to the current load step.

Increments of the rate of deformation and spin tensors are integrated using the midpoint rule to obtain the second order accuracy:

$$\Delta \boldsymbol{d} \equiv {}^{n+1/2}\boldsymbol{d}\Delta t = \left\{ \frac{\partial \Delta \boldsymbol{u}}{\partial^{n+1/2}\boldsymbol{x}} \right\}_s \qquad \Delta \boldsymbol{w} \equiv {}^{n+1/2}\boldsymbol{w}\Delta t = \left\{ \frac{\partial \Delta \boldsymbol{u}}{\partial^{n+1/2}\boldsymbol{x}} \right\}_a \tag{26}$$

where

$${}^{n+1/2}\boldsymbol{x} \equiv \frac{1}{2}({}^{n}\boldsymbol{x} + {}^{n+1}\boldsymbol{x})$$

The rotation increment $\Delta\Omega \equiv {}^{n+1/2}\Omega\Delta t$ is also evaluated using the midpoint integration of $\dot{\boldsymbol{R}} = \Omega \cdot \boldsymbol{R}$ which yields

$$\Delta\Omega \equiv {}^{n+1/2}\Omega\Delta t = ({}^{n+1}\boldsymbol{R} - {}^{n}\boldsymbol{R}) \cdot {}^{n+1/2}\boldsymbol{R}^T$$

The corotational increments of $\boldsymbol{d}$ and ω are given as

$$\Delta \boldsymbol{d}^R = {}^{n+1/2}\boldsymbol{R}^T \cdot \Delta \boldsymbol{d} \cdot {}^{n+1/2}\boldsymbol{R} \tag{27}$$

$$\Delta \omega^R = {}^{n+1/2}\boldsymbol{R}^T \cdot (\Delta \boldsymbol{w} - \Delta\Omega) \cdot {}^{n+1/2}\boldsymbol{R} \tag{28}$$

Applying the backward Euler scheme to the second equation in (13), we obtain the elastic increment of the rate of deformation as

$$\Delta_e \boldsymbol{d}^R = \frac{1}{2}(\Delta_e \boldsymbol{U} \cdot {}_e\boldsymbol{U}^{-1} + {}_e\boldsymbol{U}^{-1} \cdot \Delta_e \boldsymbol{U}) \tag{29}$$

where $\Delta_e \boldsymbol{U} \equiv {}_e\boldsymbol{U} - {}^{n}_{e}\boldsymbol{U}$. Solving (29) for ${}_e\boldsymbol{U}$ yields

$${}_e\boldsymbol{U} = 2\{{}^{n}_{e}\boldsymbol{U} \cdot (\mathbf{I} - \Delta_e \boldsymbol{d}^R)^{-1}\}_s \tag{30}$$

Integrating (22) - (24) using the backward Euler scheme gives

$${}_p\boldsymbol{d}^R = {}^{n}_{p}\boldsymbol{d}^R + \Delta\lambda \boldsymbol{P} : \xi^R \tag{31}$$

$$\alpha^R = {}^{n}\alpha^R + \frac{2(1-\beta)H}{3}\Delta\lambda \boldsymbol{P} : \xi^R \tag{32}$$

$$Y = {}^{n}Y + \beta H \Delta\, {}_p\bar{d}^R \tag{33}$$

Further substituting $\Delta_e \boldsymbol{d}^R = \Delta \boldsymbol{d}^R - \Delta_p \boldsymbol{d}^R$ and (31) into (30), yields

$${}_e\boldsymbol{U} = 2\{{}^{n}_{e}\boldsymbol{U} \cdot (\mathbf{I} - \Delta \boldsymbol{d}^R + {}^{n}_{p}\boldsymbol{d}^R + \Delta\lambda \boldsymbol{P} : \xi^R)^{-1}\}_s \tag{34}$$

Using backward Euler integration scheme for $\dot{\sigma}^R$ in (20) yields

$$\sigma^R = {}^n\sigma^R + \boldsymbol{L}^R({}_e\boldsymbol{U}) : \Delta_e\boldsymbol{d}^R + \{\boldsymbol{h}^R({}_e\boldsymbol{U}) \cdot \Delta_e\boldsymbol{e}^R\}_s \tag{35}$$

where

$$\Delta_e\boldsymbol{e}^R = \Delta_e\boldsymbol{d}^R + \Delta\omega^R - \frac{1}{2}\mathrm{tr}(\Delta_e\boldsymbol{d}^R)\mathbf{I} \tag{36}$$

The process is termed elastic if

$$\bar{\sigma}^R - Y\big|_{\Delta\lambda = 0} < 0$$

otherwise the process is plastic, which is the focus of the subsequent derivation.

Subtracting (32) from (35) we arrive at the following result

$$\boldsymbol{g} \equiv \xi^R - \boldsymbol{Q} : \boldsymbol{f} = \mathbf{0} \tag{37}$$

in which

$$\boldsymbol{Q} = \left(\mathbf{I} \otimes \mathbf{I} + \frac{2(1-\beta)H}{3}\Delta\lambda\boldsymbol{P}\right)^{-1} \tag{38}$$

$$\boldsymbol{f} = {}^n\xi^R + \boldsymbol{L}^R : \Delta_e\boldsymbol{d}^R + \{\boldsymbol{h}^R \cdot \Delta_e\boldsymbol{e}^R\}_s \tag{39}$$

It should be noted that $\boldsymbol{Q}$ in (37) is a function of ξ^R and $\Delta\lambda$. Once $\Delta\lambda$ is found, ξ^R can be solved using Newton's method as

$$\Delta\xi^{R(k+1)} = \Delta\xi^{R(k)} - \left(\mathbf{I} \otimes \mathbf{I} - \boldsymbol{Q} : \frac{\partial \boldsymbol{f}}{\partial \xi^R}\right)^{-1}\boldsymbol{g}\Big|_{\Delta\xi^{R(k)}} \tag{40}$$

where

$$\frac{\partial \boldsymbol{f}}{\partial \xi^R} = \frac{\partial \boldsymbol{f}}{\partial_e\boldsymbol{U}} : \frac{\partial_e\boldsymbol{U}}{\partial \xi^R} + \frac{\partial \boldsymbol{f}}{\partial \Delta_e\boldsymbol{d}^R} : \frac{\partial \Delta_e\boldsymbol{d}^R}{\partial \Delta_p\boldsymbol{d}^R} : \frac{\partial \Delta_p\boldsymbol{d}^R}{\partial \xi^R} \tag{41}$$

and

$$\frac{\partial \boldsymbol{f}}{\partial_e\boldsymbol{U}} = \frac{\partial \boldsymbol{L}^R}{\partial_e\boldsymbol{U}} : \Delta_e\boldsymbol{d}^R + \left\{\frac{\partial \boldsymbol{h}^R}{\partial_e\boldsymbol{U}} \cdot \Delta_e\boldsymbol{e}^R\right\}_s \tag{42}$$

$$\frac{\partial_e\boldsymbol{U}}{\partial \xi^R} = -2\Delta\lambda\{{}^n_e\boldsymbol{U} \cdot ((\mathbf{I} - \Delta_e\boldsymbol{d}^R)^{-1} \cdot \boldsymbol{P} \cdot (\mathbf{I} - \Delta_e\boldsymbol{d}^R)^{-1})\}_s \tag{43}$$

$$\frac{\partial \boldsymbol{f}}{\partial \Delta_e \boldsymbol{d}^R} = \boldsymbol{L}^R + \{\boldsymbol{h}^R \cdot (\mathbf{I} \otimes \mathbf{I})\}_s \qquad \frac{\partial \Delta_e \boldsymbol{d}^R}{\partial \Delta_p \boldsymbol{d}^R} = -\mathbf{I} \otimes \mathbf{I} \qquad \frac{\partial \Delta_p \boldsymbol{d}^R}{\partial \xi^R} = \Delta\lambda \boldsymbol{P} \tag{44}$$

The value of $\Delta\lambda$ is obtained by satisfying the consistency condition which assures that at the end of the current load step, $n+1$, the stress state lies on the yield surface. To this end (37) and (33) are substituted into the yield function (21), $\phi(\xi^R, Y) = 0$, which produces a nonlinear equation for $\Delta\lambda$. A standard Newton's method is applied to solve for $\Delta\lambda$:

$$\Delta\lambda^{(k+1)} = \Delta\lambda^{(k)} - \left(\frac{\partial \phi}{\partial \Delta\lambda}\right)^{-1} \phi \Big|_{\Delta\lambda^{(k)}} \tag{45}$$

where the right superscript in parenthesis represents the iteration count. It can be shown that the derivative $\partial\phi / \Delta\lambda$ required in (45) can be written as

$$\frac{\partial \phi}{\partial \Delta\lambda} = \frac{3}{2\bar{\sigma}^R} \xi^R : \boldsymbol{P} : \frac{\partial \xi^R}{\partial \Delta\lambda} - \frac{2}{3}\beta H Y \tag{46}$$

in which

$$\frac{\partial \xi^R}{\partial \Delta\lambda} = -\frac{2(1-\beta)H}{3}\left\{\mathbf{I} \otimes \mathbf{I} - \boldsymbol{Q} : \left(\frac{\partial \boldsymbol{f}}{\partial_e \boldsymbol{U}} : \frac{\partial_e \boldsymbol{U}}{\partial \xi^R} - \Delta\lambda \frac{\partial \boldsymbol{f}}{\partial \Delta_e \boldsymbol{d}^R} : \boldsymbol{P}\right)\right\}^{-1} \boldsymbol{Q} : \boldsymbol{P} : \xi^R$$

The converged value of $\Delta\lambda$ is then substituted into (37) from where ξ^R can be computed. Once $\Delta\lambda$ and ξ^R are known, ${}_e\boldsymbol{U}$ can be calculated using (34). Corotational stress and internal variables are found from (31) to (33) and (35). Stress and back stress are then calculated from $\sigma = \boldsymbol{R} \cdot \boldsymbol{\sigma}^R \cdot \boldsymbol{R}^T$ and $\alpha = \boldsymbol{R} \cdot \alpha^R \cdot \boldsymbol{R}^T$.

Remark: An alternative stress update procedure can be employed. After obtaining the expression for ${}_e\boldsymbol{U}$ in (34), the corotational Cauchy stress directly follows from (17). Consequently, plastic parameter $\Delta\lambda$ is calculated using the Newton method. Analogous to (39), we have

$$\boldsymbol{f} = \frac{2}{\det({}_e\boldsymbol{U})}\, {}_e\boldsymbol{U}\, \frac{\partial_e \Psi}{\partial_e \boldsymbol{U}^2}\, {}_e\boldsymbol{U} - {}^n\alpha^R$$

Numerical experiments indicate that the two procedures are comparable in terms of computational complexity and accuracy.

3.4 Consistent linearization

While integration of the constitutive equations affects the accuracy of the solution, the formation of the tangent stiffness matrix consistent with the integration procedure is essential to maintain the quadratic rate of convergence if one is to adopt the Newton method for the solution of the global nonlinear system of equations [30].

Derivation of the consistent tangent is obtained from the linearization of the incremental constitutive equation

$$\sigma^R = {}^n\sigma^R + \boldsymbol{L}^R({}_e\boldsymbol{U}) : \Delta_e\boldsymbol{d}^R + \{\boldsymbol{h}^R({}_e\boldsymbol{U}) \cdot \Delta_e\boldsymbol{e}^R\}_s \tag{47}$$

Taking the material time derivative of (47), (32) and (33) yields:

$$\dot{\sigma}^R = \left(\frac{\partial \boldsymbol{L}^R}{\partial_e \boldsymbol{U}} : {}_e\dot{\boldsymbol{U}}\right) : \Delta_e\boldsymbol{d}^R + \boldsymbol{L}^R : \Delta_e\dot{\boldsymbol{d}}^R + \left\{\frac{\partial \boldsymbol{h}^R}{\partial_e \boldsymbol{U}} : {}_e\dot{\boldsymbol{U}} \cdot \Delta_e\boldsymbol{e}^R + \boldsymbol{h}^R \cdot \Delta_e\dot{\boldsymbol{e}}^R\right\}_s \tag{48}$$

$$\dot{\alpha}^R = \frac{2(1-\beta)H}{3}(\dot{\lambda}\boldsymbol{P} : \xi^R + \Delta\lambda\boldsymbol{P} : \dot{\xi}^R) \tag{49}$$

$$\dot{Y} = \beta H\left(\frac{2\bar{\sigma}^R}{3}\dot{\lambda} + \frac{\Delta\lambda}{\bar{\sigma}^R}\xi^R : \boldsymbol{P} : \dot{\xi}^R\right) \tag{50}$$

where

$$\Delta_e\dot{\boldsymbol{d}}^R = \Delta\dot{\boldsymbol{d}}^R - \dot{\lambda}\boldsymbol{P} : \xi^R - \Delta\lambda\boldsymbol{P} : \dot{\xi}^R \tag{51}$$

$$\Delta_e\dot{\boldsymbol{e}}^R = \Delta_e\dot{\boldsymbol{d}}^R + \Delta\dot{\omega}^R - \frac{1}{2}\mathbf{tr}(\Delta_e\dot{\boldsymbol{d}}^R)\mathbf{I} \tag{52}$$

$${}_e\dot{\boldsymbol{U}} = 2\{{}^n_e\boldsymbol{U} \cdot (\mathbf{I} - \Delta_e\boldsymbol{d}^R)^{-1} \cdot \Delta_e\dot{\boldsymbol{d}}^R \cdot (\mathbf{I} - \Delta_e\boldsymbol{d}^R)^{-1}\}_s = \boldsymbol{T}^{eU} : \Delta_e\dot{\boldsymbol{d}}^R \tag{53}$$

and $\boldsymbol{T}^{eU}$ in (53) is defined as

$$T^{eU}_{ijkl} \equiv {}^n_eU_{ir}(\delta_{rk} - \Delta_e d^R_{rk})^{-1}(\delta_{lj} - \Delta_e d^R_{lj})^{-1} + {}^n_eU_{jr}(\delta_{rk} - \Delta_e d^R_{rk})^{-1}(\delta_{li} - \Delta_e d^R_{li})^{-1}$$

Details of the linearization of $\Delta\boldsymbol{d}^R$ and $\Delta\omega^R$ consistent with the integration procedures described in the previous section are given in the Appendix. The expressions for $\Delta\dot{\boldsymbol{d}}^R$ and $\Delta\dot{\omega}^R$ can be symbolically expressed as

$$\Delta\dot{\boldsymbol{d}}^R = \boldsymbol{T}^d : \boldsymbol{l} \qquad \Delta\dot{\omega}^R = \boldsymbol{T}^\omega : \boldsymbol{l} \tag{54}$$

where $\boldsymbol{T}^d$ and $\boldsymbol{T}^\omega$ are fourth order tensors derived in the Appendix ((88) and (89)).

In the case of deviatoric plasticity

$$\mathrm{tr}(\Delta_e \boldsymbol{d}^R) \;=\; \mathrm{tr}(\Delta \boldsymbol{d}^R) \qquad \text{since} \qquad \mathrm{tr}(\Delta_p \boldsymbol{d}^R) \;=\; 0 \tag{55}$$

and thus (52) can be simplified as

$$\Delta_e \dot{\boldsymbol{e}}^R \;=\; \Delta_e \dot{\boldsymbol{d}}^R + \boldsymbol{T}^e : \boldsymbol{l} \qquad \text{where} \qquad T^e_{ijkl} \equiv T^{\omega}_{ijkl} - \frac{1}{2}\delta_{ij} T^d_{ppkl} \tag{56}$$

Substituting equations (51) - (56) into (48) yields

$$\dot{\sigma}^R \;=\; \boldsymbol{A} : \Delta_e \dot{\boldsymbol{d}}^R + \tilde{\boldsymbol{A}} : \boldsymbol{l} \tag{57}$$

where

$$A_{ijkl} \equiv L^R_{ijkl} + \frac{1}{2}(\delta_{il} h^R_{jk} + \delta_{jl} h^R_{ik}) + T^{eU}_{mnkl}\left(\frac{\partial L^R_{ijpq}}{\partial_e U_{mn}} \Delta_e d^R_{pq} + \frac{\partial h^R_{ip}}{\partial_e U_{mn}} \Delta_e e^R_{pj} + \frac{\partial h^R_{jp}}{\partial_e U_{mn}} \Delta_e e^R_{pi}\right)$$

$$\tilde{A}_{ijkl} \equiv \frac{1}{2} T^e_{mnkl}(\delta_{in} h^R_{jm} + \delta_{jn} h^R_{im})$$

Subtracting (49) from (57) yields

$$\dot{\xi}^R \;=\; (\boldsymbol{A} : \boldsymbol{T}^d + \tilde{\boldsymbol{A}}) : \boldsymbol{l} + \bar{\boldsymbol{A}} : (\dot{\lambda}\xi^R + \Delta\lambda \dot{\xi}^R) \tag{58}$$

where

$$\bar{\boldsymbol{A}} \equiv \left(\boldsymbol{A} - \frac{2(1-\beta)H}{3}\mathbf{I} \otimes \mathbf{I}\right) : \boldsymbol{P}$$

Therefore, $\dot{\xi}^R$ can be written explicitly as

$$\dot{\xi}^R \;=\; \boldsymbol{T}^l : \boldsymbol{l} + \dot{\lambda} \boldsymbol{T}^{\xi} : \xi^R \tag{59}$$

in which

$$\boldsymbol{T}^l \equiv (\mathbf{I} \otimes \mathbf{I} - \Delta\lambda \bar{\boldsymbol{A}})^{-1} : (\boldsymbol{A} : \boldsymbol{T}^d + \tilde{\boldsymbol{A}}) \qquad \boldsymbol{T}^{\xi} \equiv (\mathbf{I} \otimes \mathbf{I} - \Delta\lambda \bar{\boldsymbol{A}})^{-1} : \bar{\boldsymbol{A}}$$

In order to eliminate $\dot{\lambda}$ from (48), we substitute (50) and (59) into the linearized form of the consistency condition (21)

$$\dot{\phi} \equiv \frac{3}{2\bar{\sigma}^R}\, \xi^R : \boldsymbol{P} : \dot{\xi}^R - \dot{Y} \;=\; 0$$

which yields

$$\dot{\lambda} = c\,\xi^R : \boldsymbol{P} : \boldsymbol{T}^l : \boldsymbol{l} \qquad c \equiv \left(\frac{4\beta H Y^2}{9 + 6\Delta\lambda\beta H} - \xi^R : \boldsymbol{P} : \boldsymbol{T}^{\xi} : \xi^R \right)^{-1} \tag{60}$$

Substituting (54), (59) and (60) into (51) yields

$$\Delta_e \dot{\boldsymbol{d}}^R = \boldsymbol{T}^{e d^R} : \boldsymbol{l} \tag{61}$$

where

$$\boldsymbol{T}^{e d^R} \equiv \boldsymbol{T}^d - \Delta\lambda \boldsymbol{P} : \boldsymbol{T}^l - c\{\xi^R : \boldsymbol{P} : (\mathbf{I} \otimes \mathbf{I} + \Delta\lambda \boldsymbol{T}^{\xi})\} \otimes (\boldsymbol{T}^l : \boldsymbol{P} : \xi^R)$$

The consistent linearization of σ^R is obtained by substituting (61) into (57)

$$\dot{\sigma}^R = \hat{\boldsymbol{D}} : \boldsymbol{l} \qquad \text{where} \qquad \hat{\boldsymbol{D}} \equiv \boldsymbol{A} : \boldsymbol{T}^{e d^R} + \tilde{\boldsymbol{A}} \tag{62}$$

Finally, substituting (62) and $\dot{\boldsymbol{R}} = \boldsymbol{G} : \boldsymbol{l}$ into $\dot{\boldsymbol{\sigma}} = \boldsymbol{R} \cdot \dot{\sigma}^R \cdot \boldsymbol{R}^T - \boldsymbol{R} \cdot \dot{\boldsymbol{R}}^T \cdot \boldsymbol{\sigma} - \boldsymbol{\sigma} \cdot \dot{\boldsymbol{R}} \cdot \boldsymbol{R}^T$ yields

$$\dot{\boldsymbol{\sigma}} = \boldsymbol{D} : \boldsymbol{l} \tag{63}$$

where $\boldsymbol{D}$ is the consistent stiffness tangent operator defined as

$$D_{ijkl} \equiv R_{im} \hat{D}_{mnkl} R_{jn} - R_{im} G_{nmkl} \sigma_{nj} - \sigma_{im} G_{mnkl} R_{jn} \tag{64}$$

4.0 Numerical examples

In this section we present numerical examples to study the accuracy of the proposed formulation. The $\boldsymbol{B}$-bar approach [14][16] is employed to handle the isochoric nature of plastic flow. In the following examples, the isotropic elastic strain energy density function ${}_e\Psi$ is chosen as

$${}_e\Psi = \frac{\lambda}{4}({}_eU^2_{mm} - 3)({}_eU^2_{nn} - 3) + \frac{\mu}{2}({}_eU^2_{mn} - \delta_{mn})({}_eU^2_{mn} - \delta_{mn})$$

where λ and μ are Lame constants.

4.1 Rotating-stretching shaft

In this first example, we compare the classical hypoelastic based plasticity approach to the proposed formulation for the rotating-stretching shaft problem [27]. We consider an isotropic shaft subjected to a motion whose deformation gradient is given by

$$\boldsymbol{F} = \boldsymbol{R}\boldsymbol{U} = \begin{bmatrix} \cos\theta t & -\sin\theta t & 0 \\ \sin\theta t & \cos\theta t & 0 \\ 0 & 0 & 1 \end{bmatrix} \begin{bmatrix} 1+\gamma t & 0 & 0 \\ 0 & 1 & 0 \\ 0 & 0 & 1 \end{bmatrix} \qquad t \geq 0 \tag{65}$$

The motion defined by (65) gives rise to a triaxial stress state where the principal axis is aligned with the rotating x_1-axis. We choose $\theta = \pi$ and $\gamma = 1$, so that at $t = 1$, the shaft is aligned with the global x_1-axis, and the corresponding axial component of the Lagrangian strain reaches the value of $3/2$.

Three materials with Young's modulus corresponding to soft, medium and stiff behavior were selected to study the differences between the hypoelastic and hyperelastic formulations. The following materials properties were chosen: Young's modulus (E) = 500, 3000, 20000; Poison ratio (ν) = 0.3; Y = 1000; H = 0; β = 1.

It can be easily shown that prior to yielding the corotational Cauchy stress as obtained with the two models is given as

$$\bar{\sigma}^{R}_{hypo} = \frac{E}{1+\nu}\ln(1+t) \tag{66}$$

and

$$\bar{\sigma}^{R}_{hyper} = \frac{E}{2(1+\nu)(1-2\nu)}\frac{t(2+t)\{(1-\nu)(1+t)^2-\nu\}}{(1+t)} \tag{67}$$

The two corotational effective stresses are plotted versus the axial component of Lagrangian strain (Figure 2) for the three materials considered. For the stiffest material (E=20000) the maximum elastic stretch ${}_eU_{11}$ reaches the value of 1.114 and no significant differences between the two formulations is observed. However, in the case of E=3000, the axial strain corresponding to the onset of yielding in the hypoelastic approach is 2.6 times higher than that in the present hyperelastic approach. For softer materials the difference between the two approaches becomes even more profound.

4.2 Simple shear problem

Consider the classical shear problem depicted in Figure 3. The deformation gradient is chosen as

$$\boldsymbol{F} = \begin{bmatrix} 1 & t & 0 \\ 0 & 1 & 0 \\ 0 & 0 & 1 \end{bmatrix} \qquad t \geq 0$$

Only elastic behavior is considered. Material constants considered are: E=10000, (ν) = 0.3. The corotational effective stress as obtained with the corotational hypoelastic approach employing Jaumann and Dienes rates are compared to the present approach in Figure 4. It can be seen that for small deformation only, $t < 0.4$, the three approaches produce similar elastic stretches

$$ {}_e\boldsymbol{U} = \begin{bmatrix} 1 & 0.4 & 0 \\ 0.4 & 1.16 & 0 \\ 0 & 0 & 1 \end{bmatrix} $$

The two hypoelastic models have a similar behavior up to $t < 1.5$, at which point the Jaumann formulation results in a well known oscillatory response.

4.3 Torsion of thick-walled cylinder

The geometry of the cylinder was chosen as: length = 2, inner radius = 1, outer radius = 2. Material parameters considered were: E = 21000, ν =0.3, Y = 21, H = 1000, β = 1.

All the degree of freedoms at one end were fixed, whereas at the other end appropriate displacements were prescribed to simulate free-end torsion. The finite element mesh containing 1200 8-node brick elements is shown in Figure 5. The axial strain versus the shear deformation is depicted in Figure 6. It can be seen that the maximum extension is just 0.3% while the tube is rotated by 90 degrees. This agrees well with experimental observations indicating that the axial length changes during the free-end torsion of hollow cylinders of FCC and BCC metals at room temperature are usually small for finite rotation [22].

4.4 Axisymmetric expansion of thick-walled cylinder

Axisymmetric expansion of a thick-walled cylinder is one of the most popular benchmark for validating finite plasticity formulations (see for example [28]). The configuration of the cylinder is shown in Figure 7. We consider a cylinder with inner radius of 10 and outer radius of 20 units. This problem is solved using 20 4-node bi-linear axisymmetric elements. The material parameters considered are: E = 11050, ν = 0.454, Y = 0.5, H = 0, β = 1. These values were chosen so as to replicate rigid-plastic behavior and to allow comparison with the exact solution obtained in [6]. In Figure 8 we show the relationship between the inner radius and internal pressure, and in Figure 9 we show the σ_{rr} profile versus position relative to the inner radius. It can be seen that numerical results are in good agreement with the exact solution.

5.0 Discussion

Finite deformation plasticity model based on the postulate that the corotational Cauchy stress can be derived from the Helmholtz free energy density as

$$\sigma^R = \frac{1}{\det({}_e\boldsymbol{U})}\, {}_e\boldsymbol{U}\, \frac{\partial_e \Psi}{\partial_e \boldsymbol{U}^2}\, {}_e\boldsymbol{U} \tag{68}$$

has been developed. Equation (68) is similar to the constitutive model originally proposed by Lee [20] with only exception that $\sigma^R \det({}_e\boldsymbol{U})$ is replaced by S and ${}_e\boldsymbol{U}$ by ${}_e\boldsymbol{F}$. The major difference, however, is in kinematical assumption: the model of Lee employs the multiplicative decomposition [20] whereas in the present manuscript the additive split of the rate of deformation and the absence of plastic spin are postulated.

The model has been validated on four test problems as the numerical results were found to be in good agreement with either the exact solution or experimental data. From a numerical standpoint, the proposed formulation has several advantages. On one hand it employs plasticity formulation similar to that for small deformation theory, but on the hand, the use of hyperelastic constitutive model renders the choice and numerical integration of objective stress rates entirely superfluous as the results are automatically objective. Even though we have derived an explicit expression for the tangent moduli consistent with the update strategy, the high computational cost associated with the consistent tangent evaluation might not be justified. In particular, this might be the case when multilevel methods are employed as linear solvers within the Newton method [9]. Thus in a general purpose implementation an approximation of the consistent tangent moduli or the use of quasi-Newton method might be a better choice.

References

1 *ABAQUS Theory Manual*, Version 5.4, Hibbit, Karlson & Sorensen, Inc., 1994.

2 S. N. Atluri, “An endochronic approach and other topics in small and finite deformation computational elasto-plasticity,” *Finite Element Methods for Nonlinear Problems*, Europe-US Symposium, Trondheim, Norway 1985, eds. Bergan, Bathe, Wunderlich, Springer, Berlin Heidelberg, 1986.

3 T. Belytschko, “An overview of semidiscretization and time integration procedures,” *Computational Methods for Transient Analysis*, (eds., T. Belytschko and T. J. R. Hughes), Elsevier Science Publishers, pp.1-95, 1983.

4 T. Belytschko and B. J. Hsieh, “Nonlinear transient finite element analysis with convected coordinates,” *International Journal of Numerical Methods in Engineering*, 7, 1973.

5 J. K. Dienes, “On the analysis of rotation and stress rate in deforming bodies,” *Acta Mech.*, 32, pp. 217-232, (1979).

6 D. Durban, “Large strain solution for pressurized elasto-plastic tubes,” *Journal of Applied Mechanics*, 46, 1979.

7 R. A. Eve and B. D. Reddy, “The variational formulation and solution of problems of finite-strain elastoplasticity based on the use of a dissipation function,” *International Journal of Numerical Methods in Engineering*, 37, pp.1673-1695, 1994.

8 R. A. Eve, B. D. Reddy and R. T. Rockafellar, “An internal variable theory of elasto-plasticity based on the maximum plastic work inequality,” *Quart. Appl. Math.*, 48, pp. 59-83, 1990.

9 J. Fish and K. L. Shek, “Computational Aspects of Incrementally Objective Algorithms for Large Deformation Plasticity,” *International Journal of Numerical Methods in Engineering*, in print (1998).

10 A. E. Green and P. M. Naghdi, “A general theory of an elasto-plastic continuum,” *Arch. Rat. Mech. Anal.*, 18, 1965.

11 A. E. Green and P. M. Naghdi, “Some Remarks on Elastic-Plastic Deformation at Finite Strain,” *Int. J. Engng. Sci.*, 9, pp. 1219-1229, 1971.

12 R. Hill, *The Mathematical Theory of Plasticity*, p. 23. Clarendon Press, Oxford, 1950.

13 J. V. Howard and S. L. Smith, “Recent developments in tensile testing,” *Proc. Roy. Soc. London*, A107, pp.113-125, 1925.

14 T. J. R. Hughes, “Generalization of selective integration procedures to anisotropic and nonlinear media,” *International Journal of Numerical Methods in Engineering*, 15, 1980.

15 T. J. R. Hughes, “Numerical implementation of constitutive models: Rate-independent deviatoric plasticity,” in S. Nemat-Nasser, R. J. Asaro and G. A. Hegemier, editors, *Theoretical Foundation for Large Scale Computations for Nonlinear Material Behavior*, Martinus Nijhoff Publishers, 1983.

16 T. J. R. Hughes, *The Finite Element Method: Linear Static and Dynamic Finite Element Analysis*, Prentice-Hall, 1987.

17 T. J. R. Hughes and J. Winget, “Finite rotation effects in numerical integration of rate constitutive equations arising in large deformation analysis,” *International Journal of Numerical Methods in Engineering*, 15, 1980.

18 G. C. Johnson and D. J. Bammann, “A discussion of stress rates in finite deformation problems,” *Sandia Rept.*, SAND82-8821, 1982.

19 S. J. Kim and J. T. Oden, “Finite element analysis of a class of problems in finite elastoplasticity based on the thermodynamic theory of materials of type N,” *Computer Methods in Applied Mechanics and Engineering*, 53, pp.277-302, 1985.

20 E. H. Lee, “Elastic-plastic deformations at finite strains,” *Journal of Applied Mechanics*, 36, 1969.

21 E. H. Lee, “Some comments on elastic-plastic analysis,” *Int. J. Solids Structures*, 17, pp. 859-872, 1981.

22 P. Majors and E. Krempl, “Comments on induced anisotropy, the Swift effect, and finite deformation inelasticity,” *Mechanics Research Communications*, 21, 1994.

23 B. Moran, M. Ortiz and C. F. Shih, “Formulation of implicit finite element methods for multiplicative finite deformation plasticity,” *International Journal of Numerical*

Methods in Engineering, 29, 1990.

24 L. C. Nagtegaal and J. E. De Jong, “Some computational aspects of elastic-plastic large strain analysis,” *International Journal of Numerical Methods in Engineering*, 17, pp. 15-41, 1981.

25 S. Nemat-Nasser, “Decomposition of strain measures and their rates in finite deformation elastoplasticity,” *Int. J. Solids Structures*, 15, pp. 155-166, 1979.

26 S. Nemat-Nasser, “On Finite deformation elasto-plasticity,” *Int. J. Solids Structures*, 18, pp. 857-872, 1982.

27 M. M. Rashid, “Incremental Kinematics for Finite Element Applications,” *International Journal for Numerical Methods in Engineering*, 36, pp. 3937-3956, 1993.

28 J. C. Simo, “A framework for finite strain elastoplasticity based on maximum plastic dissipation and the multiplicative decomposition. Part II: Computational aspects,” *Computer Methods in Applied Mechanics and Engineering*, 68, 1988.

29 J. C. Simo and M. Ortiz, “A unified approach to finite deformation elasto-plastic analysis based on the use of hyperelastic constitutive tensor,” *Computer Methods in Applied Mechanics and Engineering*, 49, 1985.

30 J. C. Simo and R. L. Taylor, “Consistent tangent operators for rate-independent elastoplasticity,” *Computer Methods in Applied Mechanics and Engineering*, 48, 1985.

31 A. V. Skachenko and A. N. Sporykhin, “On the additivity of tensors of strains and displacements for finite elastoplastic deformations,” *PMM*, Vol. 41, pp. 1145-1146, 1977.

32 H. Swift, “Length changes in metals under torsional overstrain,” *Engineering*, 163, pp. 253, 1947.

33 H. Zielger, “A modification of Prager’s hardening rule,” *Quarterly of Applied Mathematics*, 17, 1959.

34 A.M. Cuitino and M.Ortiz, “A material-independent method for extending stress update algorithms from small-strain plasticity to finite plasticity with multiplicative kinematics,” *Eng. Comp*., Vol. 9, pp. 437-451, 1992.

35 A.L. Eterovich and K.J.Bathe, “A hyperelastic based large strain elasto-plastic constitutive formulation with combined isotropic-kinematic hardening using logarithmic stresses and strain measures,” *International Journal for Numerical Methods in Engineering*, Vol. 30, pp. 1099-1115, 1990.

36 J.C. Simo, “Algorithms for static and dynamic multiplicative plasticity that preserve the classical return mapping schemes of the infinitesimal theory,” *Computer Methods in Applied Mechanics and Engineering*, Vol. 98, pp. 41-104, 1992.

37 J.C. Simo and T.J.R. Hughes, “Computational Inelasticity,” Springer Verlag, New York, 1998.

38 J.C. Simo and K.S.Pister, “Remarks on rate constitutive equations for finite deformation problems: computational implications,” *Computer Methods in Applied Mechanics*

and Engineering, Vol. 46, pp. 201-216, 1984.

39 G. Webber and L. Anand,"Finite deformation constitutive equations and time integration procedure for isotropic, hyperelastic-viscoplastic solids," *Computer Methods in Applied Mechanics and Engineering*, Vol. 79, pp.173-202, 1990.

Appendixes

A. Linearization of ${}^{n+1/2}\boldsymbol{R}$ and ${}^{n+1}\boldsymbol{R}$

To evaluate $\Delta\dot{\boldsymbol{d}}^{R}$ and $\Delta\dot{\omega}^{R}$ appearing in equations (51) and (52) consistent with the integration scheme employed we first focus on the consistent linearization of ${}^{n+1/2}\boldsymbol{R}$ and ${}^{n+1}\boldsymbol{R}$.

Since the consistent tangent operator is calculated at the end of load step, $n+1$, our first task consists of expressing ${}^{n+1/2}\dot{\boldsymbol{R}}$ and ${}^{n+1}\dot{\boldsymbol{R}}$ in terms of the velocity gradient at $n+1$.

For a typical time t, the velocity gradient may be written as

$$ {}^{t}\boldsymbol{l} = {}^{t}\dot{\boldsymbol{F}} \cdot {}^{t}\boldsymbol{F}^{-1} = {}^{t}\dot{\boldsymbol{R}} \cdot {}^{t}\boldsymbol{R}^{T} + {}^{t}\boldsymbol{R} \cdot {}^{t}\dot{\boldsymbol{U}} \cdot {}^{t}\boldsymbol{U}^{-1} \cdot {}^{t}\boldsymbol{R}^{T} \tag{69} $$

Pre-multiplying (69) with ${}^{t}\boldsymbol{R}^{T}$ and post-multiplying it with ${}^{t}\boldsymbol{F}$ gives

$$ {}^{t}\boldsymbol{R}^{T} \cdot {}^{t}\boldsymbol{l} \cdot {}^{t}\boldsymbol{F} = {}^{t}\boldsymbol{R}^{T} \cdot {}^{t}\dot{\boldsymbol{R}} \cdot {}^{t}\boldsymbol{U} + {}^{t}\dot{\boldsymbol{U}} \tag{70} $$

The relation between ${}^{t}\dot{\boldsymbol{R}}$ and ${}^{t}\boldsymbol{l}$ can be obtained by subtracting the transpose of (70) from the above equation

$$ {}^{t}\dot{\boldsymbol{R}} = {}^{t}\boldsymbol{G} : {}^{t}\boldsymbol{l} \tag{71} $$

where ${}^{t}\boldsymbol{G}$ is a fourth order tensor with the components given as

$$ {}^{t}G_{ijkl} = ({}^{t}R_{ir}\,{}^{t}U_{js} - {}^{t}R_{is}\,{}^{t}U_{jr})^{-1}({}^{t}R_{kr}\,{}^{t}F_{ls} - {}^{t}R_{ks}\,{}^{t}F_{lr}) \tag{72} $$

Hence, ${}^{n+1}\dot{\boldsymbol{R}}$ may be written as

$$ {}^{n+1}\dot{\boldsymbol{R}} = {}^{n+1}\boldsymbol{G} : {}^{n+1}\boldsymbol{l} \tag{73} $$

In order to derive the expression for $\overset{n+1/2}{\dot{\boldsymbol{R}}}$, we use the following relation between $^{n+1/2}\boldsymbol{l}$ and $^{n+1}\boldsymbol{l}$

$$^{n+1/2}\boldsymbol{l} = \frac{\partial^{n+1/2}\boldsymbol{v}}{\partial^{n+1/2}\boldsymbol{x}} = \frac{\partial}{\partial^{n+1/2}\boldsymbol{x}}\left\{\frac{d}{dt}\left(\frac{^{n}\boldsymbol{x} + ^{n+1}\boldsymbol{x}}{2}\right)\right\} = \frac{1}{2}\,^{n+1}\boldsymbol{l}\cdot\frac{\partial^{n+1}\boldsymbol{x}}{\partial^{n+1/2}\boldsymbol{x}}$$

Thus, $\overset{n+1/2}{\dot{\boldsymbol{R}}}$ can be written in terms of $^{n+1}\boldsymbol{l}$ as

$$\overset{n+1/2}{\dot{\boldsymbol{R}}} = {}^{n+1}\overline{\boldsymbol{G}} : {}^{n+1}\boldsymbol{l} \tag{74}$$

where

$$^{n+1}\overline{G}_{ijkl} = \frac{1}{2}\,^{n+1/2}G_{ijkm}\frac{\partial^{n+1}x_l}{\partial^{n+1/2}x_m} \tag{75}$$

B. Linearization of Δd and Δw

We start by taking the material time derivative of the gradient of the displacement increment with respect to the position vector at the mid-step (see equation (26)):

$$\frac{d}{dt}\left(\frac{\partial\Delta\boldsymbol{u}}{\partial^{n+1/2}x}\right) = \frac{\partial^{n+1}\boldsymbol{v}}{\partial^{n}\boldsymbol{x}}\cdot\frac{\partial^{n}\boldsymbol{x}}{\partial^{n+1/2}\boldsymbol{x}} + \frac{\partial\Delta\boldsymbol{u}}{\partial^{n}\boldsymbol{x}}\cdot\frac{d}{dt}\left(\frac{\partial^{n}\boldsymbol{x}}{\partial^{n+1/2}\boldsymbol{x}}\right) \tag{76}$$

The second term in the right hand side of (76) can be written as

$$\frac{d}{dt}\left(\frac{\partial^{n}\boldsymbol{x}}{\partial^{n+1/2}\boldsymbol{x}}\right) = -\frac{\partial^{n}\boldsymbol{x}}{\partial^{n+1/2}\boldsymbol{x}}\cdot\frac{d}{dt}\left(\frac{\partial^{n+1/2}\boldsymbol{x}}{\partial^{n}\boldsymbol{x}}\right)\cdot\frac{\partial^{n}\boldsymbol{x}}{\partial^{n+1/2}\boldsymbol{x}} \tag{77}$$

Combining (76) and (77) gives

$$\frac{d}{dt}\left(\frac{\partial\Delta\boldsymbol{u}}{\partial^{n+1/2}x}\right) = \frac{\partial^{n+1}\boldsymbol{v}}{\partial^{n+1/2}\boldsymbol{x}} - \frac{\partial\Delta\boldsymbol{u}}{\partial^{n+1/2}\boldsymbol{x}}\cdot\frac{d}{dt}\left(\frac{\partial^{n+1/2}\boldsymbol{x}}{\partial^{n}\boldsymbol{x}}\right)\cdot\frac{\partial^{n}\boldsymbol{x}}{\partial^{n+1/2}\boldsymbol{x}} \tag{78}$$

Equation (78) can be further simplified by exploiting the following relation

$$\frac{d}{dt}\left(\frac{\partial^{n+1/2}\boldsymbol{x}}{\partial^{n}\boldsymbol{x}}\right) = \frac{\partial}{\partial^{n}\boldsymbol{x}}\left(\frac{d}{dt}{}^{n+1/2}\boldsymbol{x}\right) = \frac{\partial}{\partial^{n}\boldsymbol{x}}\left\{\frac{d}{dt}\left(\frac{{}^{n}\boldsymbol{x} + {}^{n+1}\boldsymbol{x}}{2}\right)\right\} = \frac{1}{2}\frac{\partial^{n+1}\boldsymbol{v}}{\partial^{n}\boldsymbol{x}}$$

which after substitution into (78) yields

$$\frac{d}{dt}\left(\frac{\partial\Delta\boldsymbol{u}}{\partial^{n+1/2}\boldsymbol{x}}\right) = \left(\mathbf{I} - \frac{1}{2}\frac{\partial\Delta\boldsymbol{u}}{\partial^{n+1/2}\boldsymbol{x}}\right)\cdot\frac{\partial^{n+1}\boldsymbol{v}}{\partial^{n+1/2}\boldsymbol{x}} \tag{79}$$

Equation (79) can be recast into the following form:

$$\frac{d}{dt}\left(\frac{\partial\Delta\boldsymbol{u}}{\partial^{n+1/2}\boldsymbol{x}}\right) = \boldsymbol{M} : \boldsymbol{l} \qquad \text{where} \qquad M_{ijkl} \equiv \frac{\partial^{n}x_i}{\partial^{n+1/2}x_k}\frac{\partial^{n+1}x_l}{\partial^{n+1/2}x_j} \tag{80}$$

by utilizing the following equality

$$\mathbf{I} - \frac{1}{2}\frac{\partial\Delta\boldsymbol{u}}{\partial^{n+1/2}\boldsymbol{x}} = \frac{\partial}{\partial^{n+1/2}\boldsymbol{x}}\left({}^{n+1/2}\boldsymbol{x} - \frac{1}{2}\Delta\boldsymbol{u}\right) = \frac{\partial^{n}\boldsymbol{x}}{\partial^{n+1/2}\boldsymbol{x}}$$

The final expressions for $\Delta\dot{\boldsymbol{d}}$ and $\Delta\dot{\boldsymbol{w}}$ can be obtained by substituting (80) into the definition of $\Delta\dot{\boldsymbol{d}}$ and $\Delta\dot{\boldsymbol{w}}$:

$$\Delta\dot{\boldsymbol{d}} \equiv \frac{d}{dt}\left\{\frac{\partial\Delta\boldsymbol{u}}{\partial^{n+1/2}\boldsymbol{x}}\right\}_s = \tilde{\boldsymbol{M}} : \boldsymbol{l} \qquad \text{where} \qquad \tilde{M}_{ijkl} \equiv \frac{1}{2}(M_{ijkl} + M_{jikl}) \tag{81}$$

$$\Delta\dot{\boldsymbol{w}} \equiv \frac{d}{dt}\left\{\frac{\partial\Delta\boldsymbol{u}}{\partial^{n+1/2}\boldsymbol{x}}\right\}_a = \hat{\boldsymbol{M}} : \boldsymbol{l} \qquad \text{where} \qquad \hat{M}_{jikl} \equiv \frac{1}{2}(M_{ijkl} - M_{jikl}) \tag{82}$$

C. Linearization of $\Delta\boldsymbol{d}^R$ and $\Delta\omega^R$

After consistently linearizing ${}^{n+1/2}\boldsymbol{R}$, ${}^{n+1}\boldsymbol{R}$, $\Delta\dot{\boldsymbol{d}}$ and $\Delta\dot{\boldsymbol{w}}$ in the Appendixes A and B, we now proceed with the linearization of $\Delta\boldsymbol{d}^R$ and $\Delta\omega^R$.

Consider equations (27), (28) and

$$\Delta\boldsymbol{d}^R = {}^{n+1/2}\boldsymbol{R}^T\cdot\Delta\boldsymbol{d}\cdot{}^{n+1/2}\boldsymbol{R}$$

$$\Delta\omega^R = {}^{n+1/2}\boldsymbol{R}^T \cdot (\Delta\boldsymbol{w} - \Delta\Omega) \cdot {}^{n+1/2}\boldsymbol{R}$$

$$\Delta\Omega = ({}^{n+1}\boldsymbol{R} - {}^{n}\boldsymbol{R}) \cdot {}^{n+1/2}\boldsymbol{R}^T$$

Taking the material time derivative of the above equations yields

$$\Delta\dot{\boldsymbol{d}}^R = {}^{n+1/2}\boldsymbol{R}^T \cdot \Delta\dot{\boldsymbol{d}} \cdot {}^{n+1/2}\boldsymbol{R} + 2\left\{ {}^{n+1/2}\boldsymbol{R}^T \cdot \Delta\boldsymbol{d} \cdot {}^{n+1/2}\dot{\boldsymbol{R}} \right\} \tag{83}$$

$$\Delta\dot{\omega}^R = {}^{n+1/2}\boldsymbol{R}^T \cdot (\Delta\dot{\boldsymbol{w}} - \Delta\dot{\Omega}) \cdot {}^{n+1/2}\boldsymbol{R} + 2\left\{ {}^{n+1/2}\boldsymbol{R}^T \cdot (\Delta\boldsymbol{w} - \Delta\Omega) \cdot {}^{n+1/2}\dot{\boldsymbol{R}} \right\} \tag{84}$$

$$\Delta\dot{\Omega} = {}^{n+1}\dot{\boldsymbol{R}} \cdot {}^{n+1/2}\boldsymbol{R}^T + ({}^{n+1}\boldsymbol{R} - {}^{n}\boldsymbol{R}) \cdot {}^{n+1/2}\dot{\boldsymbol{R}}^T \tag{85}$$

Combining (73), (74), (82) and (85) results in the following relation

$$\Delta\dot{\boldsymbol{w}} - \Delta\Omega = \overline{\boldsymbol{M}} : \boldsymbol{l} \tag{86}$$

where

$$\overline{M}_{ijkl} = \hat{M}_{ijkl} - G_{imkl}\,{}^{n+1/2}R_{jm} - ({}^{n+1}R_{im} - {}^{n}R_{im})\overline{G}_{jmkl}$$

Substituting (74), (81), (82) and (86) into (83), (84) yields

$$\Delta\dot{\boldsymbol{d}}^R = \boldsymbol{T}^d : \boldsymbol{l} \qquad \Delta\dot{\omega}^R = \boldsymbol{T}^{\omega} : \boldsymbol{l} \tag{87}$$

where

$$T^d_{ijkl} = {}^{n+1/2}R_{ri}M_{rskl}\,{}^{n+1/2}R_{sj} + \Delta d_{rs}({}^{n+1/2}R_{ri}\overline{G}_{sjkl} + {}^{n+1/2}R_{sj}\overline{G}_{rikl}) \tag{88}$$

$$T^{\omega}_{ijkl} = {}^{n+1/2}R_{ri}\overline{M}_{rskl}\,{}^{n+1/2}R_{sj} + \Delta\omega_{rs}({}^{n+1/2}R_{ri}\overline{G}_{sjkl} + {}^{n+1/2}R_{sj}\overline{G}_{rikl}) \tag{89}$$

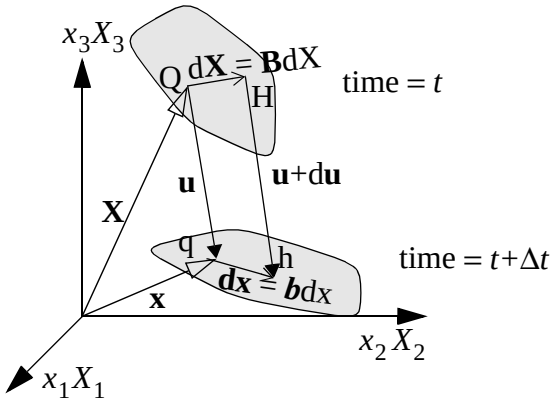

FIGURE 1. Definition of deformation gradient

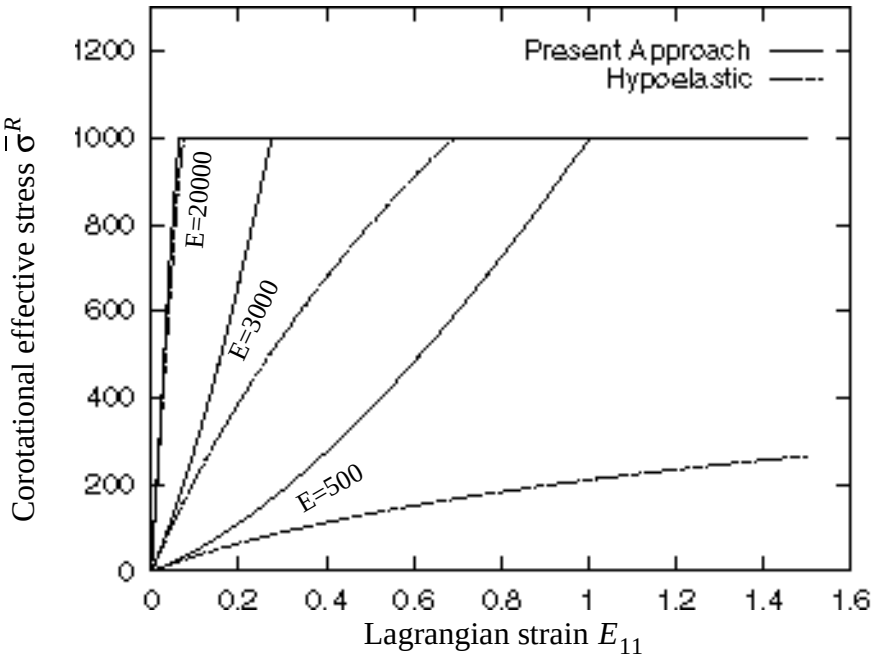

FIGURE 2. Corotational effective stress for the rotating-stretching shaft problem

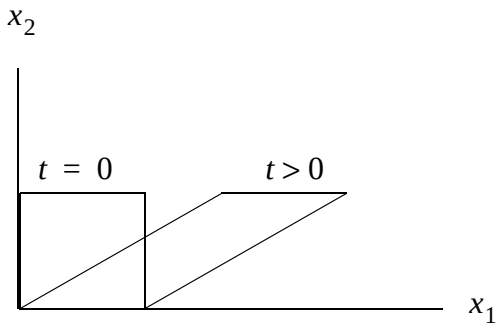

FIGURE 3. Simple shear in x_1 direction

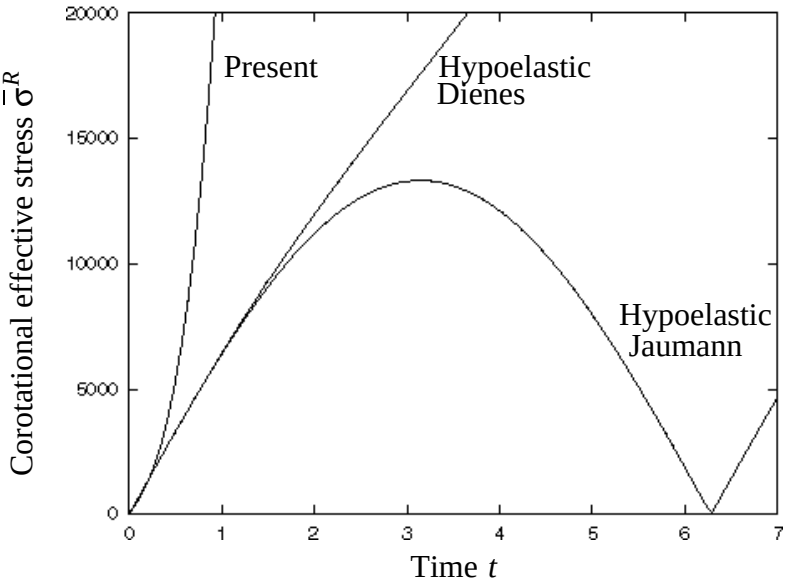

FIGURE 4. Corotational effective stress for the simple shear problem

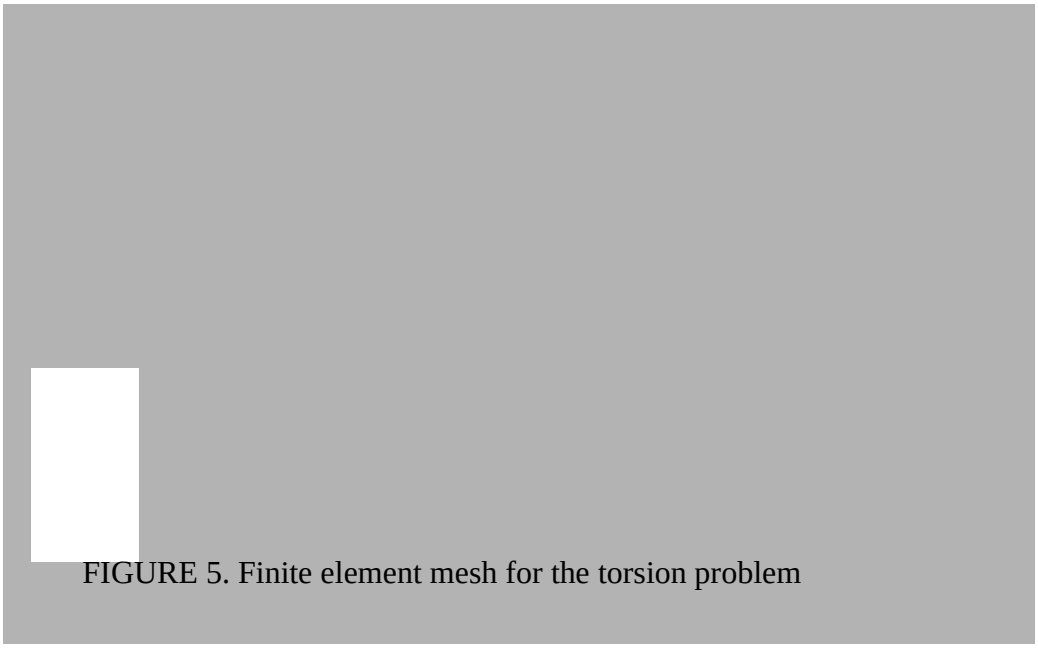

FIGURE 5. Finite element mesh for the torsion problem

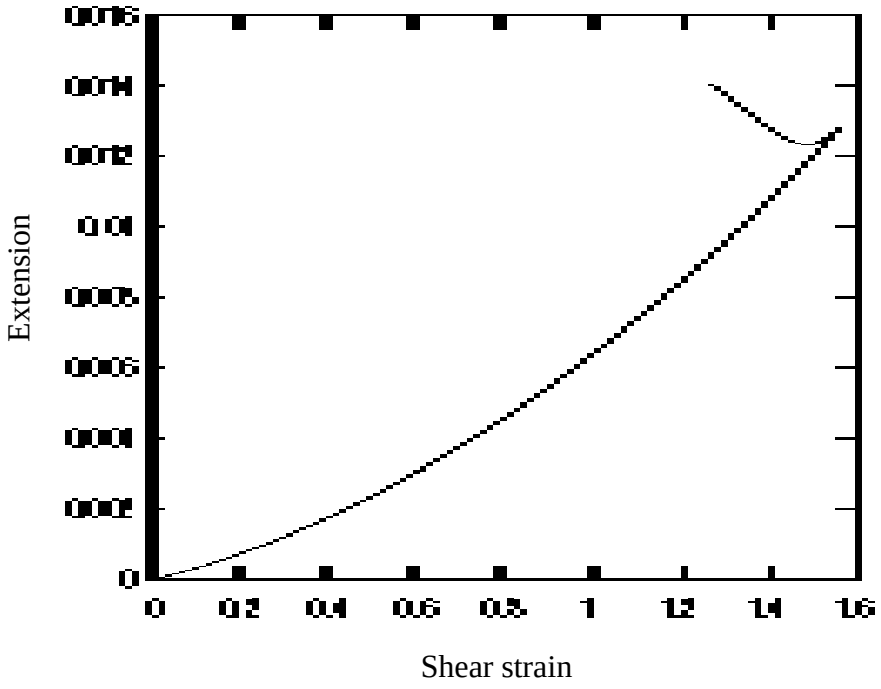

FIGURE 6. Torsion of a hollow cylinder

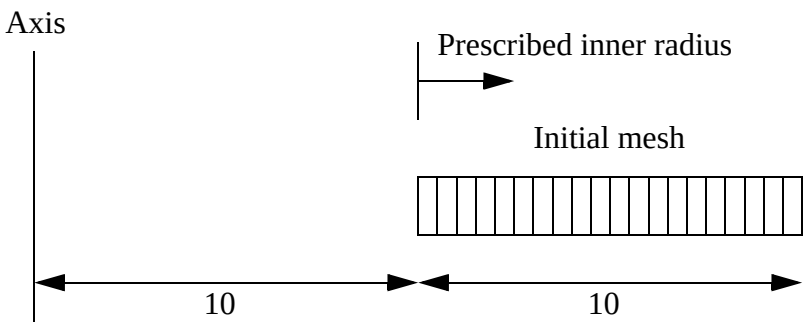

FIGURE 7. Geometry and mesh of the thick-walled cylinder

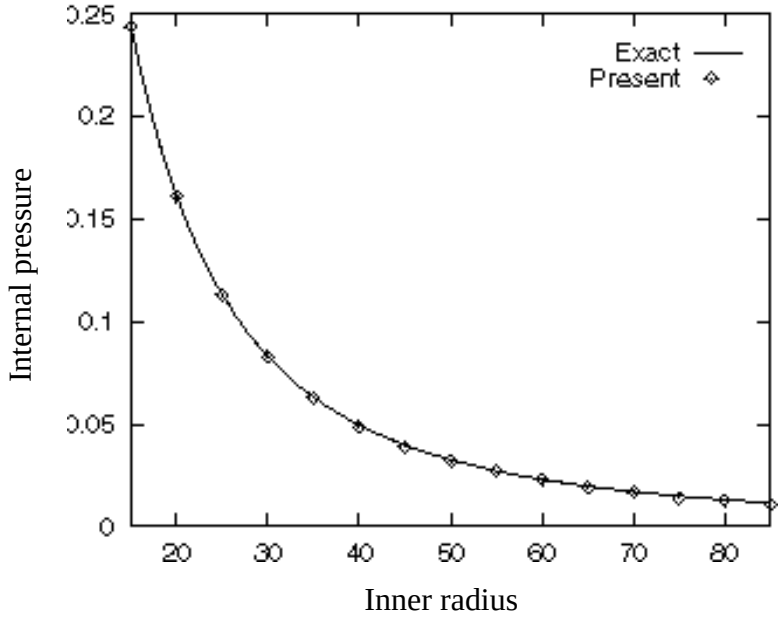

FIGURE 8. Internal pressure versus inner radius

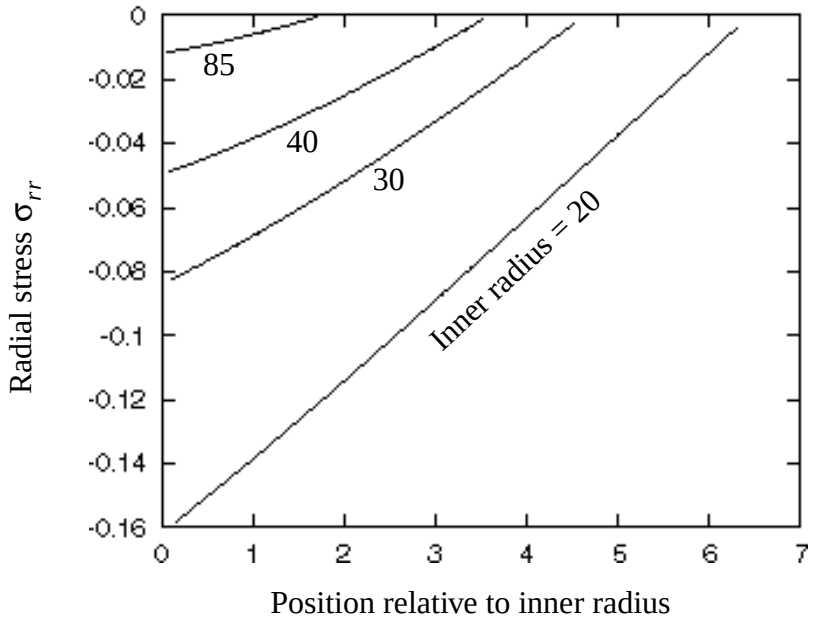

FIGURE 9. Radial stress versus position relative to inner radius